Int. J. Heat Mass Transfer. Vol. 12, pp. 749–752. Pergamon Press 1969. Printed in Great Britain

SHORTER COMMUNICATION

NATURAL CONVECTION FROM A HORIZONTAL CYLINDER AT MODERATE GRASHOF NUMBERS

J. A. PETERKA and P. D. RICHARDSON
Center for Fluid Dynamics, Division of Engineering, Brown University, Providence, Rhode Island

(*Received* 29 *July* 1968 *and in revised form* 8 *November* 1968)

NOMENCLATURE

- F_i, dimensionless stream functions;
- G_i, dimensionless temperature profiles;
- g, acceleration due to gravity;
- R, cylinder radius;
- r, radius at a point in the fluid surrounding cylinder;
- T, temperature; T_w, at wall; T_∞, far from cylinder;
- u, azimuthal velocity;
- v, radial velocity;
- β, buoyancy;
- ζ, dimensionless radial coordinate;
- η, $\zeta - Gr^{\frac{1}{4}}$;
- θ, dimensionless temperature;
- ν, kinematic viscosity;
- ξ, transformed azimuthal coordinate;
- σ, dimensionless radial coordinate;
- ϕ, azimuthal angle, measured from bottom of cylinder;
- Ψ, stream function;
- Gr, Grashof number, based on R;
- Pr, Prandtl number.

INTRODUCTION

NATURAL convection from horizontal circular cylinders at moderate Grashof numbers exhibits considerable departures from the flow and heat transfer predicted by boundary-layer analysis. These departures are caused predominantly by boundary-layer curvature which is ignored in the asymptotic ($Gr \to \infty$) analyses, these being cast in rectangular curvilinear coordinates, e.g. Hermann, Chiang and Kaye [1, 2]. In addition, some terms in the basic equations are neglected in boundary-layer analysis. For boundary-layer analysis of convection round the circular cylinder, the expansion into successive pairs of simultaneous equations as described by Chiang and Kaye [2] is convenient to use, and the convergence scheme of Nachtsheim and Swigert [3] permits solution for any Prandtl number of interest through use of a digital computer.

No analyses have been presented for moderate Grashof numbers, although some approximations have been made. For example, Elenbaas [4] adapted an early suggestion of Langmuir [5] in which a layer of fluid around the cylinder was considered stationary, with heat transfer occurring through the annular ring of fluid by conduction. Senftleben [6] proposed another approximate scheme. However, neither represents a physically correct solution. The proper formulation of the problem requires solution of the two-dimensional Navier–Stokes and energy equations, expressed most conveniently in cylindrical coordinates. These give rise to a momentum equation of higher order than that which comes from boundary-layer theory and this complicates computation of solutions because it requires a larger number of boundary values at the cylinder surface to be found by iteration.

We present here a set of solutions for the basic pair of simultaneous equations for natural convection on a horizontal cylinder. In addition, we provide comparison of the temperature profile with experiments for a Grashof number about 10^3, and comparison also with heat-transfer measurements in this region.

ANALYSIS

The Navier–Stokes equations in cylindrical coordinates (r, z, ϕ) are described by Schlichting [7]. The present problem is two-dimensional and the equation for the z-direction is neglected. For the remaining equations the pressure terms can be eliminated by cross-differentiation and subtraction of the ϕ and r equations, after multiplication of the ϕ-momentum equation by r. An appropriate stream function can be introduced, i.e. $v = -(1/r)\,(\partial\Psi/\partial\phi)$, $u = (\partial\Psi/\partial r)$. In addition, $T = \theta(T_\omega - T_\infty) + T_\infty$. The Navier–Stokes equations, including the effect of buoyancy, are then reduced to

$$u\frac{\partial}{\partial\phi}(\nabla^2\Psi) + rv\frac{\partial}{\partial r}(\nabla^2\Psi) = r\nu\nabla^4\Psi + g\beta\left(\cos\phi\frac{\partial\theta}{\partial\phi} + r\sin\phi\frac{\partial\theta}{\partial r}\right)(T_\omega - T_\infty). \quad (1)$$

This partial differential equation can be solved by first writing the velocity and temperature fields as azimuthal series of

functions of the radial coordinate r. For the asymptotic, boundary-layer solution for the horizontal cylinder, two different azimuthal series have been introduced. Chiang and Kaye [2] used a Blasius-style transformation and series: for the dimensionless radial coordinate

$$\zeta = Gr^{\frac{1}{4}} r/R,$$

the stream function

$$\Psi = \nu Gr^{\frac{1}{4}}\{\phi F_1(\zeta) + \phi^3 F_3(\zeta) + \dots\},$$

and the temperature

$$\Theta = G_0(\zeta) + \phi^2 G_2(\zeta) + \dots.$$

Saville and Churchill [8] introduced Goertler-style transformations for the same problem with

$$\xi = \int_0^{\phi} [\sin\phi]^{\frac{1}{4}}\,\mathrm{d}\phi$$

$$\sigma = (\tfrac{3}{4})^{\frac{1}{4}} \frac{rGr^{\frac{1}{4}}[\sin\phi]^{\frac{1}{4}}}{R\xi^{\frac{1}{4}}}$$

$$\Psi = (\tfrac{4}{3})^{3/4}\,\nu Gr^{1/4}\{\xi^{3/4}F_0(\sigma) + \xi^{9/4}F_1(\sigma) + \dots\}$$

$$\Theta = G_0(\sigma) + \xi^{\frac{3}{2}}G_1(\sigma) + \dots.$$

For both styles of transformation, the solution of the simultaneous partial differential equations is reduced to the successive solution of a set of simultaneous pairs of ordinary differential equations. In both cases the first pair of ordinary differential equations is dominant and represents the major portion of the complete solution even at two radians round from the bottom. With the Blasius style transformation, the lead term (i.e. the solution of the first pair of equations) gives a uniform heat-transfer rate around the cylinder, but with the Goertler form the leading term gives a local heat-transfer rate which changes slowly with azimuthal angle. While the former is a good approximation for the cylinder, the latter is even better and makes the leading term more strongly dominant. It happens that with both styles of transformation, the first pair of ordinary differential equations is the same. The solution of this pair of equations, common to both formulations, can be interpreted physically in two different ways. In the present case, we have approached the first pair of ordinary differential equations using a Blasius-style transformation and corresponding notation with subscripts omitted; in this way, the Navier–Stokes equations reduce to

$$F^{iv} + [2/\zeta]F''' - [1/\zeta^2]F'' + [1/\zeta^3]F' - [Gr^{\frac{1}{4}}/\zeta^2]F'^2 - [Gr^{\frac{1}{4}}/\zeta]F'F'' - [Gr^{\frac{1}{4}}/\zeta^3]FF' + [Gr^{\frac{1}{4}}/\zeta^2]FF'' + [Gr^{\frac{1}{4}}/\zeta]FF''' + G' = 0. \quad (2)$$

The energy equation in cylindrical coordinates can be expressed in terms of the same variables as

$$G'' + [1/\zeta]G' + [Gr^{\frac{1}{4}}/\zeta]\,Pr\,FG' = 0. \quad (3)$$

The known boundary conditions are $F = 0$, $F' = 0$, $G = 1$ at $r = R$ i.e. $\zeta = Gr^{\frac{1}{4}}$; $F' \to 0$, $F'' \to 0$, $G \to 0$ as $r \to \infty$.

In the process of solution, the three boundary values

$$F'', F''' \quad \text{and} \quad G' \quad \text{at} \quad r = R$$

must be found. This can be accomplished by iteration with a digital computer by seeking values which simultaneously make F', F'', F''', G and G' become very close to zero at a sufficiently large value of ζ, integration of equations (2) and (3) being carried out by a fourth-order Runge–Kutta program. Convergence for this problem proves to be far more tedious than for the limiting case of boundary-layer flow where only two boundary values need to be found. A list of values computed for $Pr = 0{\cdot}72$ is given in Table 1. In addition, some graphs have been prepared which illustrate how the solutions depart from the boundary-layer limit. In these graphs the coordinate $\eta = \zeta - Gr^{\frac{1}{4}}$ (i.e. the non-dimensional distance from the wall) has been used.

Figure 1 illustrates the temperature profiles for a range of Grashof numbers down to 10^3. There is remarkably little difference which can be seen between these: but when the temperature gradient profiles are examined, Fig. 2, it can be seen that there are indeed marked differences at small values of η. As the Grashof number is reduced the gradient at the cylinder surface increases, as does the curvature of the temperature profile (G'''). The increase in the dimensionless heat transfer rate (proportional to G' at $r = R$) as Gr decreases corresponds to relatively increased flow, as seen in Fig. 3.

The equations above do reduce to those for a boundary layer as $Gr \to \infty$, of course, if the transformation $\eta = \zeta - Gr^{\frac{1}{4}}$ is used.

COMPARISON WITH EXPERIMENTS

Measurements of temperature and velocity profiles have been reported in the literature, but these appear to be of indifferent accuracy or have suffered in reproduction so that comparison cannot be made with sufficient precision. However, we had available some schlieren-interferometer photographs of isotherms around a cylinder as part of the results from an investigation of the effects of sound on natural convection. Figure 4 shows a comparison of the temperature profile as determined from the interference fringe positions (circles), the present analysis (solid line) for the conditions of the experiment ($Gr = 1380$), and analysis for $Gr \to \infty$ (dashed line). The comparison is very favorable. Further interferographs, for other Grashof numbers, processed so as to estimate the local heat transfer at the bottom of a heated cylinder were compared with the analysis and found to lie within the experimental uncertainty, i.e. ± 4 per cent. The measured values are listed in Table 2. The increase in heat transfer, above the expectation from the limiting solution for $Gr \to \infty$, that is predicted by the analysis for finite Grashof numbers is closely matched by measurements of

Table 1. Boundary values

Gr	F''	F'''	G'	G' (approximation equation (4))
∞	0·8560	−1·0000	−0·3741	−0·3741
1×10^8	0·8775	−1·0342	−0·3800	−0·379
1×10^7	0·8944	−1·0614	−0·3846	−0·383
1×10^6	0·9246	−1·1109	−0·3927	−0·390
1×10^5	0·9791	−1·2026	−0·4068	−0·402
3×10^4	1·0236	−1·2798	−0·4179	−0·411
1×10^4	1·0785	−1·3780	−0·4311	−0·423
6×10^3	1·1099	−1·4357	−0·4385	−0·429
3×10^3	1·1612	−1·5313	−0·4504	−0·439
$1{\cdot}38 \times 10^3$	1·2306	−1·6655	−0·4657	−0·452
1×10^3	1·2639	−1·7317	−0·4729	−0·459

overall heat transfer. The velocity measurements of Jodlbauer [9] include Grashof numbers in the range 8000 to 600,000. It is probable that these measurements are closer to the total velocity, $(u^2 + v^2)^{\frac{1}{2}}$, than to the azimuthal velocity. When the measurements are compared with the analysis given here the agreement is quite good even at 90° round the cylinder from the bottom, and beyond. This serves to illustrate the dominance of the solution of the first pair of equations, as mentioned previously, well away from the bottom.

DISCUSSION

If Langmuir's method is adapted to provide approximate predictions of the effect of boundary layer curvature as used for forced convection by Richardson [10], this indicates that

$$G' = -0{\cdot}3741\{1 + 1{\cdot}33Gr^{-\frac{1}{4}} - 0{\cdot}357Gr^{-\frac{1}{2}} + \ldots\}. \quad (4)$$

Values given by this expression have been entered in the right-hand column of Table 1. The values given by equation (4) are within 3 per cent of the correct values. This indicates that equation (4) is a useful approximation for heat transfer; of course, it provides no information about the corresponding flow. The values support the observation that departures from the asymptotic value for heat transfer are caused predominantly by boundary layer curvature. The departures are quite large: for a Grashof number of 10^3 the increase in heat transfer is nearly 30 per cent. The results have practical significance because the difference between the complete and the boundary-layer solutions becomes comparable with typical experimental uncertainty (± 4 per cent, say) at a Grashof number which is not small (about 10^6). Many

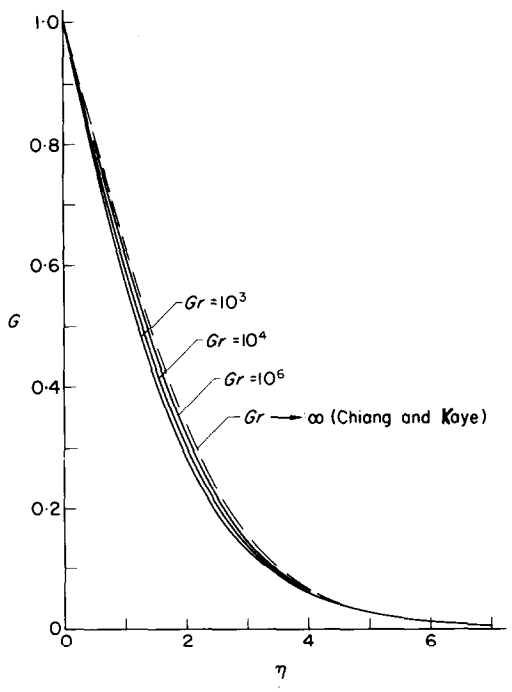

FIG. 1. Temperature profiles at the bottom of a horizontal cylinder at finite Grashof numbers.

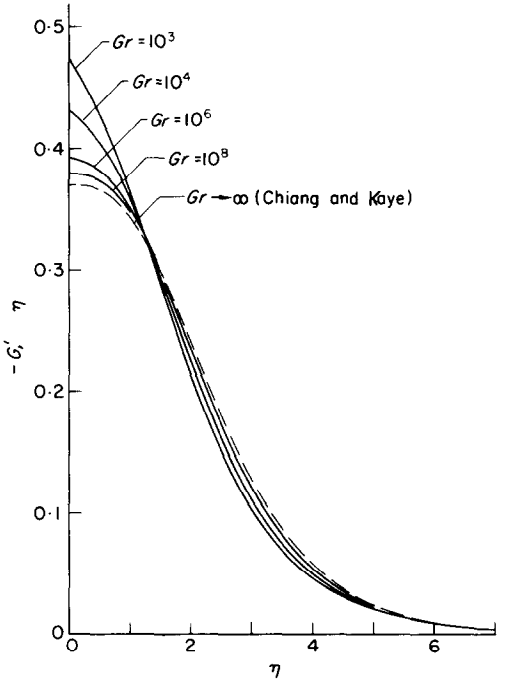

FIG. 2. Temperature gradient profiles at the bottom of a horizontal cylinder at finite Grashof numbers.

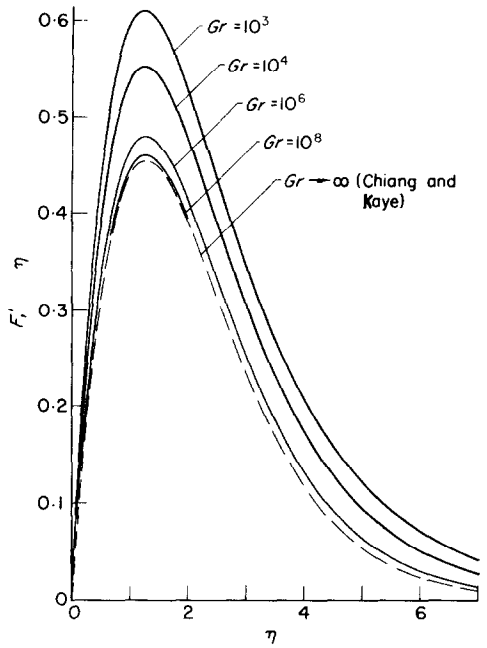

FIG. 3. Profiles of azimuthal velocity at finite Grashof numbers.

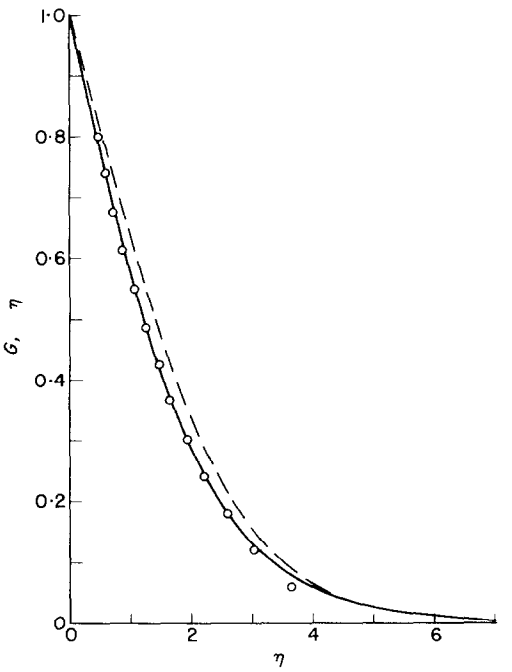

FIG. 4. Comparison between temperature profiles as determined from interference fringe positions (circles), present analysis (solid line) and boundary-layer analysis (dashed line).

Table 2

Gr	G'_{wall} Analytical	G'_{wall} Experimental	Difference (per cent)
$1{\cdot}38 \times 10^3$	$-0{\cdot}466$	$-0{\cdot}473$	$+1{\cdot}5$
$2{\cdot}12 \times 10^3$	$-0{\cdot}457$	$-0{\cdot}448$	$-2{\cdot}0$
$2{\cdot}59 \times 10^3$	$-0{\cdot}453$	$-0{\cdot}462$	$+2{\cdot}0$
$3{\cdot}00 \times 10^3$	$-0{\cdot}450$	$-0{\cdot}433$	$-3{\cdot}8$

experiments and applications occur with smaller Grashof numbers.

REFERENCES

1. R. HERMANN, Heat transfer by free convection from horizontal cylinders in diatomic gases, *NASA Rep. No.* TM 1366 (1954).
2. T. CHIANG and J. KAYE, On laminar free convection from a horizontal cylinder, *Proc.* 4th *U.S. Natl. Congr. Appl. Mech.* 1213 (1962).
3. P. R. NACHTSHEIM and P. SWIGERT, Satisfaction of asymptotic boundary conditions in numerical solution of systems of equations of boundary-layer type, *NASA Rep. No.* TN D-3004 (1965).
4. W. ELENBAAS, The dissipation of heat by free convection from vertical and horizontal cylinders, *J. Appl. Phys.* **19**, 1148 (1948).
5. I. LANGMUIR, Convection and conduction of heat in gases, *Phys. Rev.* **34**, 401 (1912).
6. H. SENFTLEBEN, Die Wärmeabgabe von Körpern verschiedener Form in Flüssigkeiten und Gasen bei freier Strömung, *Z. Angew. Phys.* **3**, 361 (1951).
7. H. SCHLICHTING, *Boundary Layer Theory* (Translated by J. KESTIN), Chap. 3, McGraw-Hill, New York (1960).
8. D. A. SAVILLE and S. W. CHURCHILL, Laminar free convection in boundary layers near horizontal cylinders and vertical axisymmetric bodies, *J. Fluid Mech.* **29**, 391 (1967).
9. K. JODLBAUER, Das Temperatur- und -Geschwindigkeitsfeld um ein geheiztes Rohr bei freier Konvektion, *Forsch. Geb. IngWes.* Vol. 4, 157 (1933).
10. P. D. RICHARDSON, Convection from heated wires at moderate and low Reynolds numbers, *AIAA Jl.* **3**, 537 (1965).

ACKNOWLEDGEMENTS

The computations were supported by NSF Grant GP-4825. The measurements used for comparison were performed in connection with part of the research program of heat transfer in unsteady flows of the Aeronautical Research Laboratories, Office of Aerospace Research of the U.S. Air Force. This support is gratefully acknowledged.